

**ASYNCHRONOUS TRAVELING-WAVE INDUCED LINEAR MOTION OF LIVING
CELLS**

**FUHR, G.(1); HAGEDORN, R.(1); MÜLLER, T.(1); BENECKE, W.(2);
WAGNER; B.(2); and GIMSA; J.(1)**

(1) Humboldt-Universität zu Berlin, Fachbereich Biologie

(2) Fraunhofer-Institut für Mikrostrukturtechnik, Berlin

An electrodynamic traveling-wave induced linear transfer of dielectric particles such as living cells and artificial objects of microscopic dimensions is described. Various configurations of microelectrodes obtained by microfabrication techniques were realized on silicon or glass substrates. For an effective manipulation of particles immersed in weak electrolyte solutions (i) electrode geometries corresponding with particle size and (ii) high frequency traveling-waves have to be used. The motion of particles can be characterized as traveling-wave dielectrophoresis (TWD). Microparticle velocities of some hundred $\mu\text{m/s}$ have been achieved applying phase-shifted rectangular pulses with amplitudes between 4 and 15 volts. A theoretical estimation of the particle motion is given.

Introduction

Alternating electric fields are well suited for manipulation and characterization of living cells. They have been used for a large number of applications such as cell to cell fusion / 15 /, dielectric single cell spectroscopy / 1,3 /

and, more or less effective, cell separation procedures by means of dielectrophoresis / 11 /. The main advantage using alternating fields is the existence of a frequency range (1 kHz ... 1 GHz) with minimal loading of cells. However, procedures for linear translation of cells as a supposition for manipulation and cell separation are less developed up to now. One technique is named dielectrophoresis where cells are attracted or repelled from points of high field strength. Since these points are determined by the electrode configuration a flexible particle handling is restricted. Additionally, at a given frequency no reversal of the particle movement can be achieved. As another possibility high frequency rotating fields can be used to induce cell rolling on smooth surfaces (agar) in vertical-arranged four electrode chambers / 4 /. This principle is less effective due to liquid streaming effects and the hindrance of rolling cells by particles fixed on the surface.

These investigations and the similarity to traveling-wave induced pumping of liquids as described by MELCHER / 10 / twentyfive years ago, enforced us to develop arrays of electrodes for a linear displacement of particles.

This paper describes principles of field generation and electrode arrangements for unidirectional propagation of dielectric particles in comparison to electrorotation / 3 /. The appropriate microelectrode structures were fabricated on silicon or glass substrates using standard IC fabrication techniques. Among others sure translocation of living suspended cells through complex microstructures opens up completely new possibilities to investigate, transform and

separate single cells.

Materials and Methods

1. Electrode configurations

The microelectrode structures were fabricated on quartz glass as well as on oxidized silicon wafers as starting material. After deposition of a Cr/Au plating base a photoresist with a thickness up to 25 μm was deposited and lithographically structured. The electrodes were formed by electroplating of gold up to a thickness of 20 μm . After removal of the photoresist ion milling was used to etch the plating base.

High frequency traveling-waves were applied to the electrode configurations shown in Fig.1a and b.

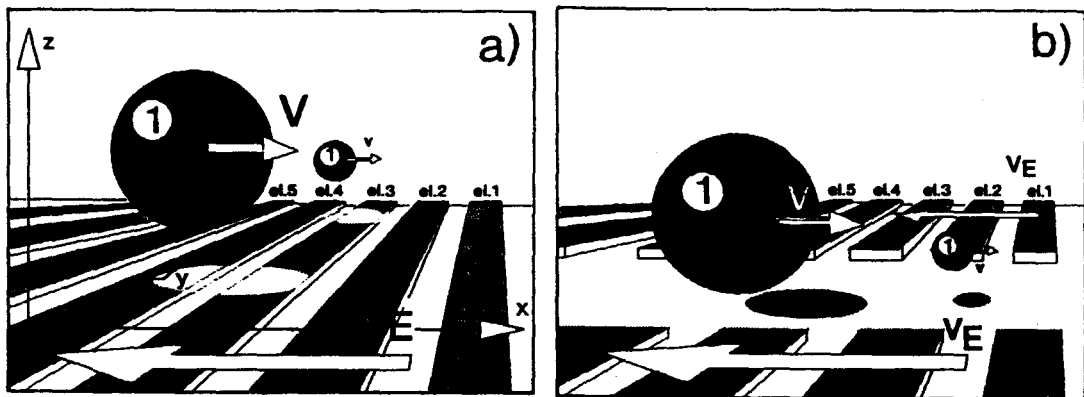


FIG.1a

Schematic structure of a microelectrode array:
 1 - dielectric particles levitated and driven as denoted
 by arrows with a velocity (v)
 el 1..5 - electrode strips
 V_E - direction and velocity of the traveling-wave

FIG.1b

Structure with interelectrode gap and dielectric particles (1) focused and levitated within the electrode free space. Traveling-waves on both sides induce contrary motion of particles

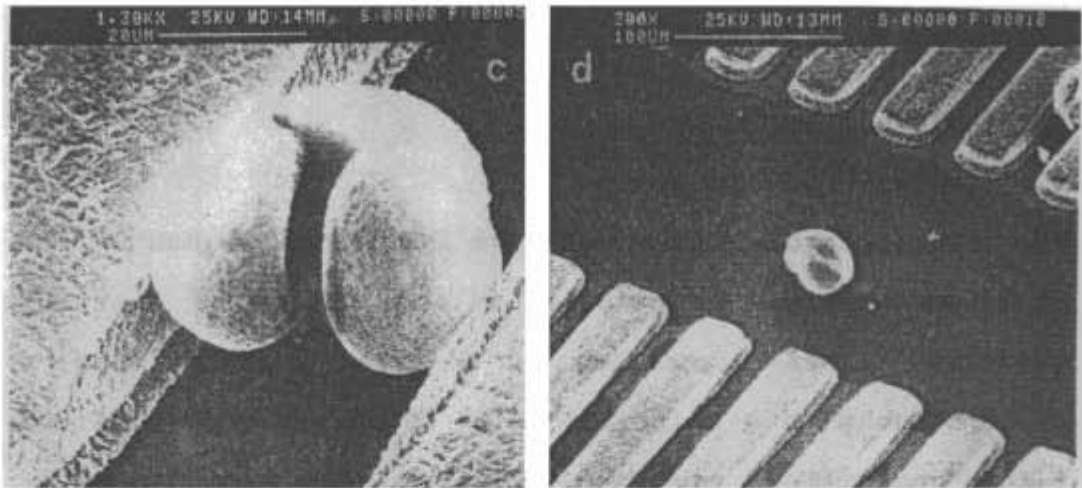
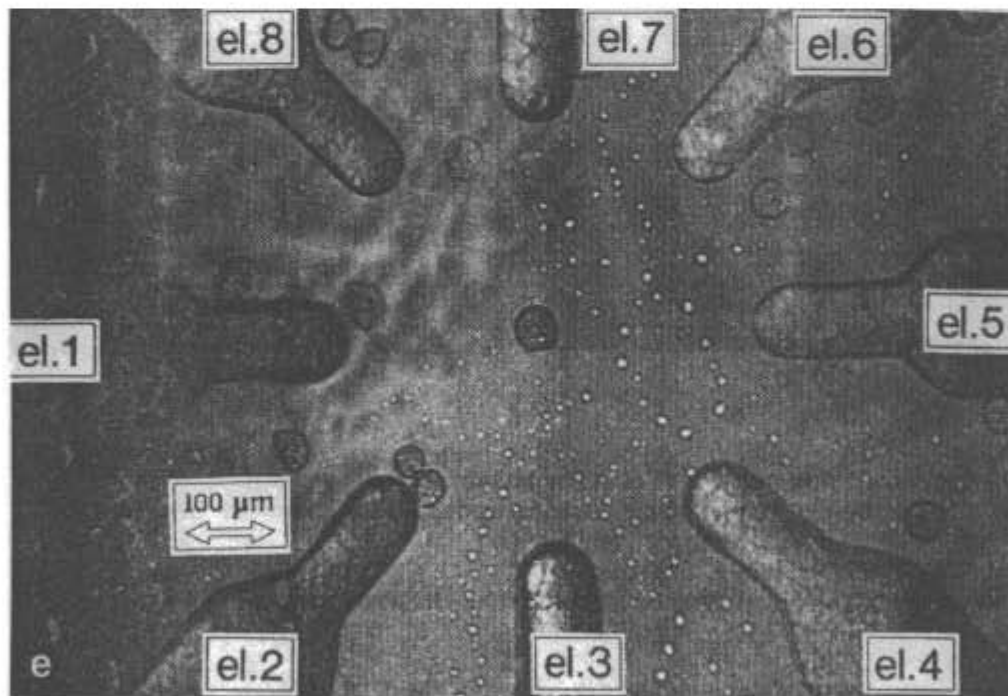


FIG.1c

SEM photograph of the surface of a microchamber with pollen (*Pinus sylvestris*) between electrodes

FIG.1d

SEM photograph of the interelectrode gap with pollen (*Pinus sylvestris*)



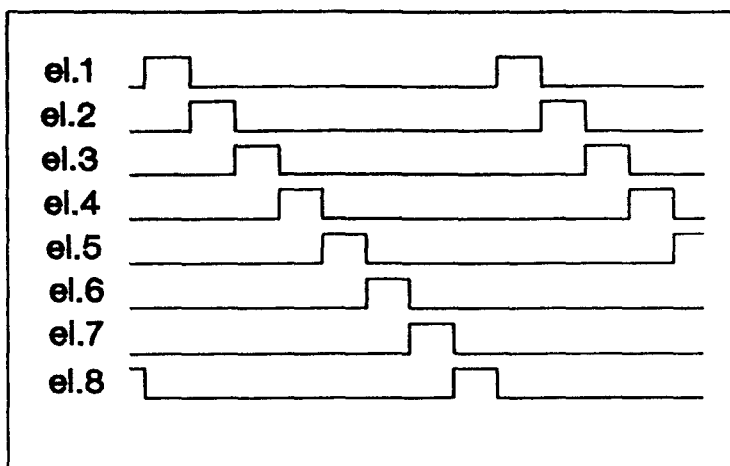


FIG.1e
Eight-electrode chamber (gold on quartz glass) with cells (pollen of *Populus tremula*) suspended in water to create rotating electric field induced spinning of cells. The time flow of the output voltages applied to the electrodes is shown additionally.

Rotation of cells was studied with rotating electric fields in eight-electrode chambers applying 45° phase-shifted rectangular pulses (Fig.1e). The angular frequency of the field could be varied between 100 Hz and 32 MHz. For more details of electrorotation see / 1,3 /.

2. Electric field generation

Traveling fields were generated by supplying neighbouring electrodes with 90° phase-shifted pulse sequences of 4-15 V amplitude. In Figs.2a and b the excitation sequence for four successive time intervals is shown. The resulting field travels from the top to the bottom as shown in Fig.2. Since the field is generated by (n) phase-shifted waves the phase velocity (V_E) is given by:

$$V_E = n (x_{el} + x_{in}) * f \quad (1)$$

where

f is the frequency of the alternating field

x_{el} is the width of electrodes

x_{in} is the distance between the electrodes

n is the number of phase shifted pulse sequences

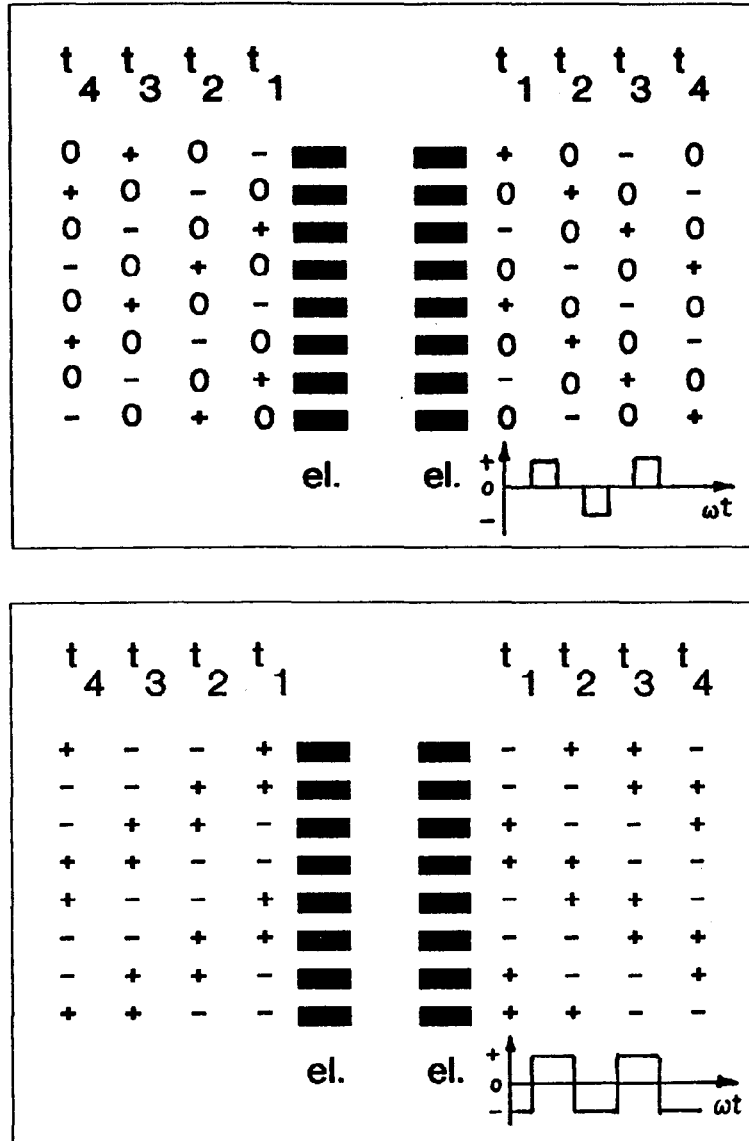


FIG.2

Polarity of electrodes producing traveling-waves using 90° phase-shifted pulse sequences

a) rectangular tri-state excitation

b) rectangular two-state excitation

$t_{1..4}$ - time

el - electrodes

Within the frequency range used (100Hz - 100MHz) the wave phase propagates in the described structures with a velocity of

between 0.04 and $4 \cdot 10^4$ m/s. As shown in Fig.3 at even that velocity also the points of field minima propagate. This is the most important difference from conventional dielectrophoresis.

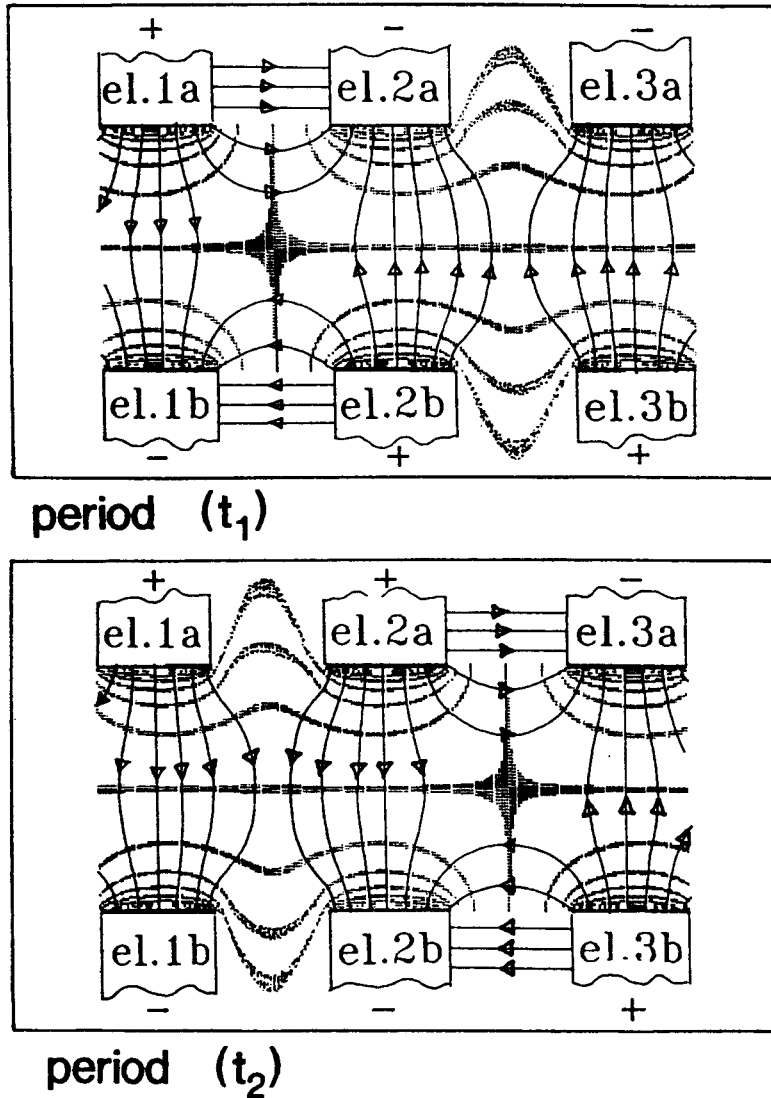


FIG.3
 Electric field lines (—) and equipotential lines (::::) within an interelectrode gap created by high frequency traveling-waves of opposite polarity according to Fig.2b
 a) period (t_1)
 b) period (t_2), the field has moved one step to the right hand side

3. Dielectric particles

For an efficient manipulation the dielectric particles

should exhibit the following properties:

- Particle size and electrode geometries correspond in their dimensions;

- Particles differ in their physical properties

(dielectric constant, conductivity) from the surrounding

medium which in biological relevant cases has to be water.

Most animal and plant cells having diameters between 1 and several hundred micrometers fulfil both presumptions. The behaviour of yeast cells (*Saccharomyces cerevisiae*) and pollen (*Populus tremula*, *Pinus sylvestris*, *Pseudotsuga menziesii*) has been studied. All cells were suspended in weak electrolyte solutions (conductivity between 1 and 30 mS/m) as commonly used for physiological experiments.

As artificial objects cellulose-disulphate spheres (diameter 5 - 100 μm) were investigated.

Theoretical background

Three kinds of electrical effects act on a dielectric particle exposed to high frequency electric fields:

1. Orientation in the case of non-spherical geometry or asymmetrical dielectric composition of the particle;
2. Forces resulting from asymmetrical polarization in non-uniform fields and temporal displaced charges (dielectrophoresis);
3. Forces due to temporary but also spatial displaced image charges (e. g. by a constant angle in the case of spinning dielectrics in rotating fields or by a constant distance in the case of traveling fields).

Additionally, two types of polarization, apoelectric and paraelectric polarization / 11 /, should be distinguished (Fig.4).

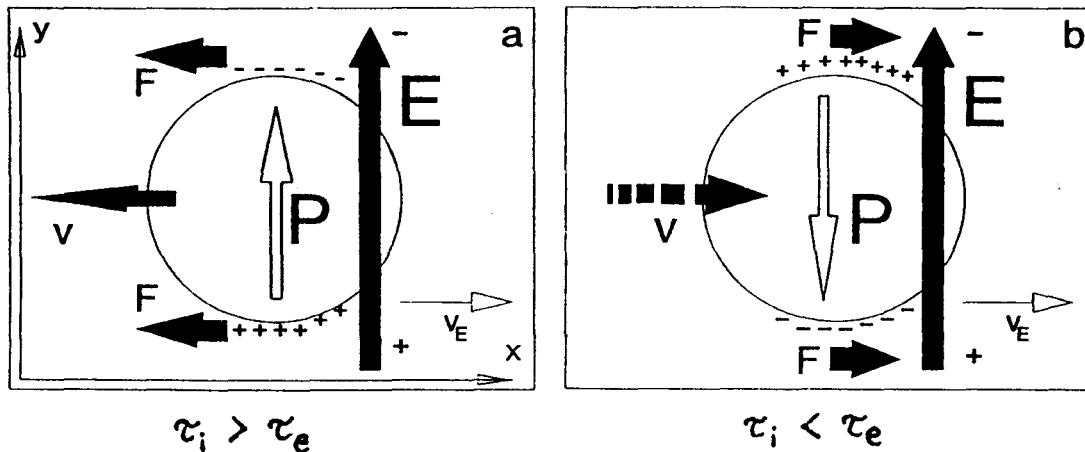


FIG.4a
 Electric field vector (E) traveling across a homogeneous dielectric particle with velocity (v_E) and position of the induced dipole moment (P) describing the localization of imaged charges (+,-). The force (F) leads to particle motion (v) contrary to the field vector (apoelectric polarization)

FIG.4b
 Paraelectric polarization of the particle and forces acting in direction of the traveling field
 $\tau_i = \epsilon_i / G_i$ and $\tau_e = \epsilon_e / G_e$ are relaxation times (i- sphere, e- external medium)

The particle movement is explained in the following:

The electric field vector (E_y) causes a polarization vector (p_y) which is also orientated in the y-direction. If the field vector is moved perpendicular to its orientation (e. g. in x-direction) there will be a spatial delay between field and polarization vector. This delay causes either repulsion between the polarization charges and the field vector (apoelectric case; $E_y * p_y > 0$; Fig.4a) or attraction (paraelectric case; $E_y * p_y < 0$; Fig.4b).

If the delay between the exciting field and the polarization vector becomes zero than also the driving forces vanish. The delay and the driving forces reach a

maximum if the relaxation time for the polarization charges corresponds to this time the field phase needs pass the particle. The main difference from conventional dielectrophoretic motion of particles is the coupling of the relaxation effects with the phase velocity of the traveling field. For this reason the motion induced by TWD and the rotation in rotating fields are physically similar. In contrast to rotating fields which can be homogeneous, the non-uniform character of traveling-waves complicates the situation due to effects which are proportional to the gradient of the field strength (repulsion or attraction of the particle towards the electrodes superimposed to the linear driving force). As a result the behaviour of dielectrics exposed to traveling-waves is more complex than electrorotation. Especially the configuration of electrodes and their geometry play an important role. A short derivation considering a typical arrangement of electrodes excited by rectangular pulses is given in the Appendix. Note that each configuration of electrodes requires a separate calculation. The understanding of the linear motion described needs some additional remarks:

The net linear motion of cells is a complex superposition of linear driving forces, dielectrophoretic forces, frictional forces (in the solution and on surfaces) and the torque leading to cell rotation. Except the linear driving forces acting on microparticles, all effects were separately investigated in detail /3,5,6,10,11,13/. Fundamental works were done by LAMPA (rotation of particles / 7 /), MELCHER (traveling-wave induced pumping / 10 /), JONES (levitation

of particles / 5 /) and POHL (dielectrophoresis / 11 /). Low frequency traveling-waves (several Hz) and their influence on liquid immersed cells were first investigated by MASUDA et al. / 8,9 /, however, considering only permanent surface charges and applying low frequencies (0.1 ...100 Hz). Therefore, in this paper we give an estimation for the linear driving force (see Appendix) and develop the real motion of particles by superposition with the remaining effects. The general interaction between the driving forces and dielectrophoresis is illustrated in Fig.5:

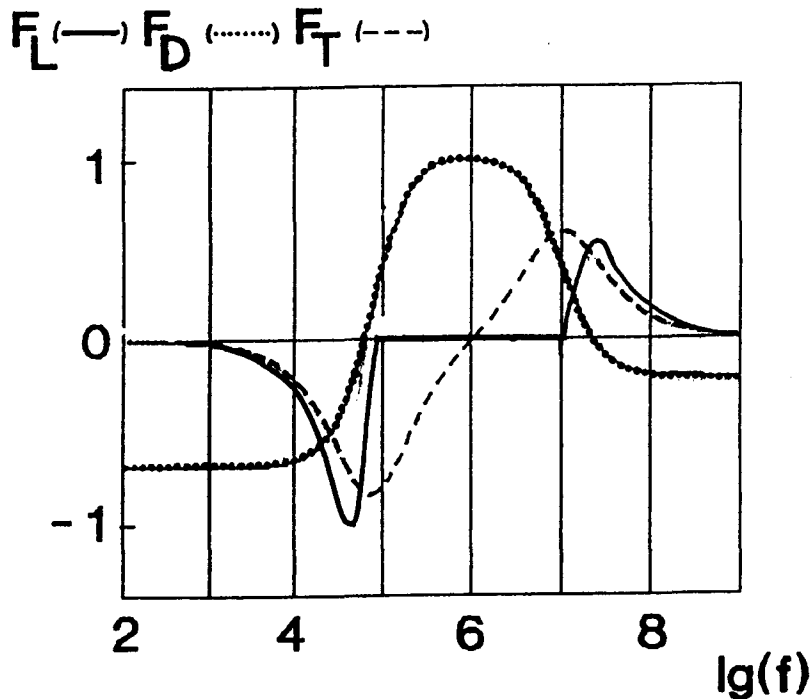


FIG.5
Forces as a function of frequency (f) leading to linear motion of a cell which is assumed to be a single-shelled dielectric sphere.

F_D - dielectrophoretic force

F_T - translational force

F_L - resulting force reflecting the real linear motion of cells

Without dielectrophoresis the linear motion of a cell would follow the dashed line in Fig.5 which is a result of the

linear driving force only. Additionally forces arise from dielectrophoresis (dotted line). These forces are either directed towards the electrode surfaces (frequency range of positive dielectrophoresis) or in the reverse direction (negative dielectrophoresis). In the first case the cell is pressed onto the electrode surface and frictional forces suppress any transversal motion. In the second case the cell is levitated into free solution and the linear driving force becomes effective. The interplay of both forces leads to the real motion (thick line).

Results

a) Linear motion of homogeneous spheres:

As a model object for homogeneous particles cellulose-disulfate spheres of about 60 μm diameter were used. The spheres were either immersed in a medium of high conductivity (first case) or low conductivity (second case). Electrorotation as well as linear movement have been measured.

In the first case (Figs. 6a-d) the conductivity of the fluid was adjusted to have negative dielectrophoretic forces (Fig. 6d) within the whole frequency range. As a consequence, the particle is levitated and its motion (Fig. 6a) is determined by the linear driving forces only (Fig. 6c, for a derivation see Appendix). The experimentally determined curve agrees well with the calculated one. The velocity-frequency plot in Fig. 6b shows that electrorotation

and linear cell motion are very similar effects. This could be expected because in both cases the same relaxation processes determine the driving forces.

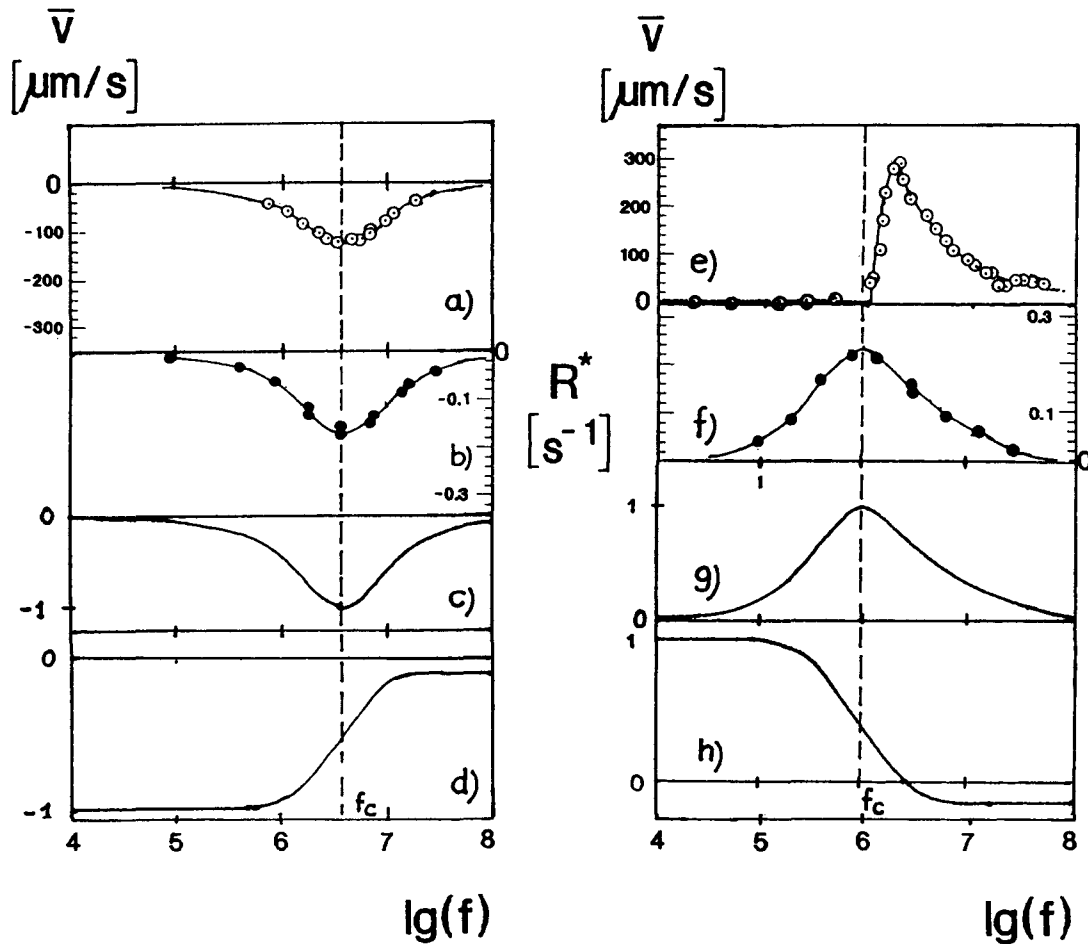


FIG.6
 Average velocity (\bar{v}) of linear motion of a cellulose-disulfate sphere (o) induced by traveling-waves and rotation (R^*) (●) of the same sphere induced by rotating fields as a function of the field frequency (f)
 left side : external conductivity $2.1 \cdot 10^{-2}$ S/m
 right side: external conductivity 10^{-3} S/m
 a,e - velocity of translation measured
 b,c - electrorotation measured
 c,g - lateral forces calculated
 d,h - dielectrophoretic forces calculated
 parameters: conductivity of the sphere: $8 \cdot 10^{-3}$ S/m
 dielectric constant : 70
 radius : $3 \cdot 10^{-5}$ m

The conductivity was chosen to have positive

dielectrophoretic force below frequencies of about 10^6 Hz (Fig.6h): Within this frequency range the cells are attracted to the electrode surface and linear motion is suppressed. As a consequence, cell motion occurs only above a frequency of 10^6 Hz due to linear driving forces (Fig. 6g); at lower frequencies frictional forces stop any motion. Therefore, the electrorotational behaviour (Fig. 6f) and the linear translation (Fig. 6e) are quite different characteristics.

b) Motion of living cells:

In a simple approach living cells can be described as single shell spheres (membrane and interior). As discussed above the measured linear motion of a cell (Fig.7a, open circles) should follow its rotational behaviour (calculated electrorotation: Fig.7b, solid line; measured electrorotation: Fig.7a, full points). The linear motion differs significantly from the rotation due to dielectrophoresis (see Fig.7b, (dashed line)). Between 10^5 and 10^7 Hz dielectrophoresis is sufficiently positive. Within this frequency range the cells are attracted by the electrodes and thus translation is suppressed.

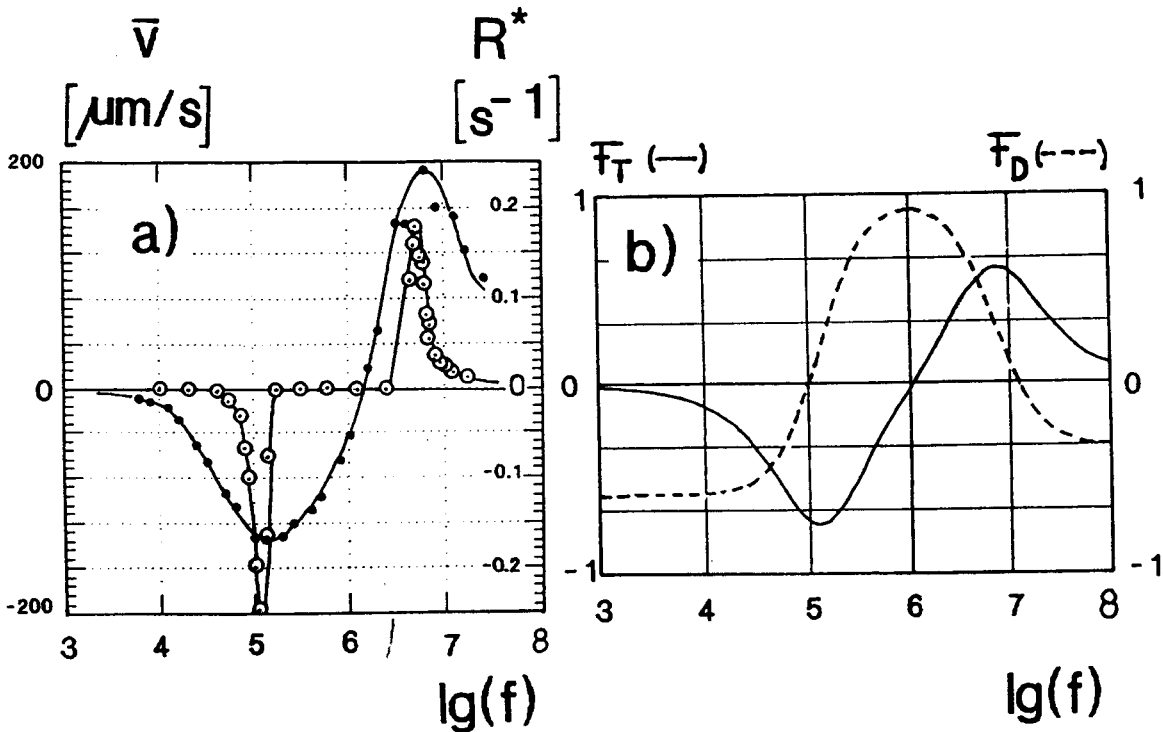


FIG.7a
 Rotation (R^*) (●) and average velocity (\bar{v}) (o) of pollen (*Pinus sylvestris*) as a function of the field frequency (f) (external conductivity: 10^{-2}S/m)

FIG.7b
 Simulation of dielectrophoresis (---) and the torque leading to rotation respectively translational force (—) using a single-shell sphere model.

Set of parameters: sphere

interior: dielectric constant	50
conductivity	10^{-1}S/m
membrane: dielectric constant	8
conductivity	10^{-7}S/m
external medium: dielectric constant	80
conductivity	10^{-2}S/m
radius:	$4 \cdot 10^{-5}\text{m}$

A more elaborated illustration of the effects is given in Fig.8:

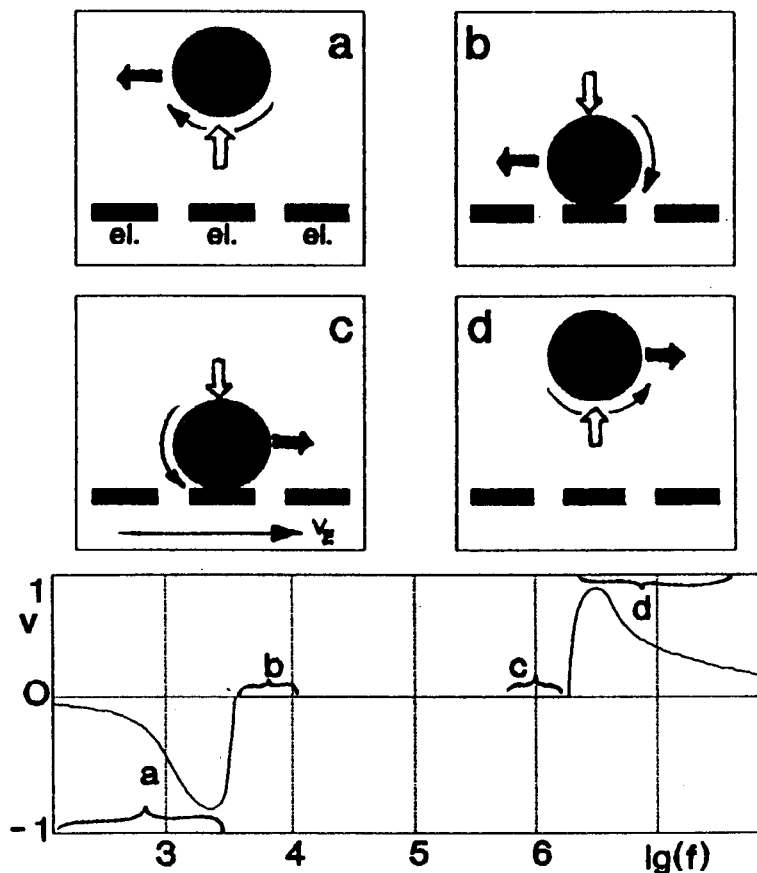


FIG. 8

Upper part: schematic cross section demonstrating the superposition of forces

- dielectrophoretic force (\Rightarrow) (in dependence on the configuration of the electrodes also in x- and y-direction)
- translational force (\rightarrow)
- torque leading to rolling (\curvearrowright)

el - electrodes

v_e - direction and velocity of the traveling-wave

lower part: Velocity of linear motion as a function of the frequency (f) of the traveling wave.

An electric field traveling from the left to the right is considered. The appropriate force vectors are shown in the Figs. 8a-d, (arrow (\Rightarrow)) represents the dielectrophoretic force, arrow (\rightarrow) denotes the lateral force as considered in the Appendix, arrow (\curvearrowright) is the torque due to electrorotation which occurs if the field vector and the polarization vector are not in parallel). Within the

frequency range (a) an anti-field propagation of cells is observed. Furthermore, dielectrophoresis is negative and causes levitation. The frictional forces are only those of a moving sphere in free solution. Within the frequency range (b) also an anti-field motion occurs but the dielectrophoretic force becomes positive and presses the cells onto the electrode surface. The net movement is an overlay between the lateral driving force which cause the cell to slide along the surface to the left hand side, and the rolling movement which displaces the cell to the left hand side. In the frequency region (c) the situation is the same as in Fig. 8b except that the motion now is a co-field motion and the direction of translation and rolling are reversed. Within the frequency range (d) the situation is as in region (a) except that co-field motion reverses the direction of the forces denoted by arrows () and ().

c) Linear motion over electrodes and within the interelectrode gap

Artificial particles as well as living cells move more continuous over electrodes than within the interelectrode gap (Fig.9). In the microstructure shown in Fig.1b, particles move slowly between the electrodes and reach a maximum between two neighbouring pairs of electrodes. This is caused by the non-uniform field distribution in x-direction (see Fig.3).

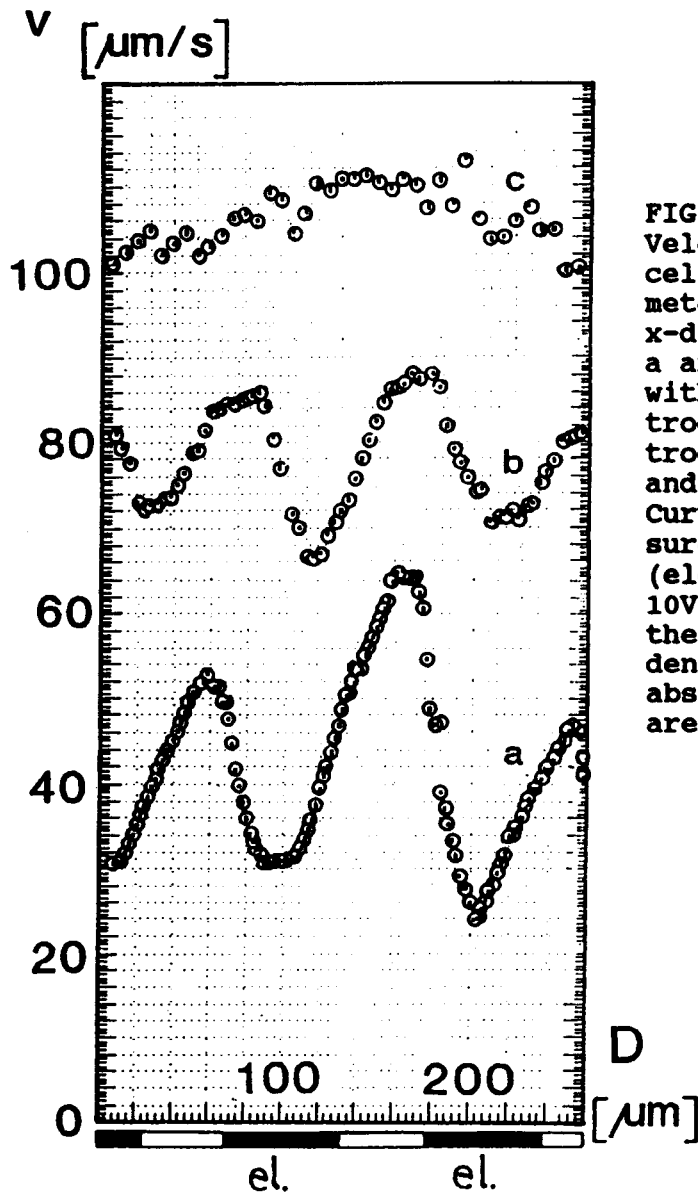


FIG.9

Velocity (v) of a cellulose sphere (diameter $60 \mu\text{m}$) in x-direction. The curve a and b are measured within the interelectrode gap with electrode voltages of 5V and 10V, respectively. Curve c has been measured over electrodes (electrode voltage 10V). The position of the electrodes is denoted below the abscissa by black areas

From theoretical point of view (see Appendix) the average force $\langle F_x \rangle$ and velocity $\langle v \rangle$, respectively, at a given position of the particle are proportional to the square of the field strength (E). However, the measured data indicate another functional dependence. This is caused by the levitation which lifts the particle towards regions of lower

field strength.

d) Focusing and transversal propagation of droplets of non-mixing liquids

Since particles can also be droplets of liquids the technique described can also be applied to emulsions. Experiments with dextrane-water droplets in 50% n-propanole showed that small droplets were focused towards minima of the electric field and fuse there to larger droplets which could be laterally moved or held in a fixed position. These results suggest technical applications such as liquid pumping or positioning of smallest volumes for chemical reactions or fixing of droplets with diameters of several micrometers to measure their properties (electrically or by combination with other techniques).

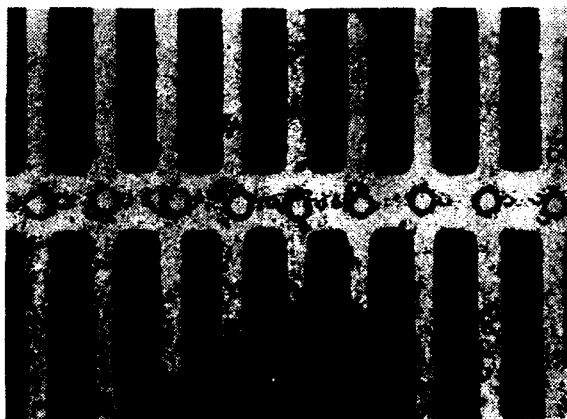


Fig.10
Water-dextrane droplets
focused towards field
minima within the inter-
electrode gap in n-pro-
panole

Discussion

Microstructured multi-electrode configurations are excellently suited for the creation of high frequency traveling-waves.

Linear motion of cells suspended in weak electrolyte solutions was tested within microelectrode strips arranged in a planar configuration or bounding an interelectrode channel. Velocities of cells between $5 \mu\text{m/s}$ and 0.5 mm/s could be achieved applying 90° phase-shifted rectangular pulses with amplitudes of 4 ... 15 V.

The effect of linear cell motion is similar to the principle of liquid pumping described by MELCHER and CROWLEY in their pioneering papers / 2,10 /. Additionally, particles are freely moveable in liquids and therefore rotate, roll on surfaces or were focused towards minima and maxima of the field, respectively. The superposition of all forces, which show a complex dependence on the external field frequency, leads to sharper peaks of the velocity of cells as a function of the frequency as measured in the case of electrorotation / 1,3 /. In a broad frequency range cells are fixed on the surface. The behaviour of particles exposed to traveling-waves (artificial as well as living cells) can be used to develop a large scale of applications:

1. Contactless manipulation of particles in microstructures;
2. Focusing and fixing of particles in electrical field traps;
3. Positioning of particles with submicron accuracy;
4. Separation of particles exhibiting different dielectric properties;
5. Fixing of particles in free solution and rotation around any axis.

Spatially arranged electrodes can be used to construct two or three dimensional configurations enclosing channels,

reaction volumes or forming cascades and filters. The technique describing TWD induced particle motion offers practicable ways to develop more complex micromechanical structures for extremely miniaturized measuring systems, manipulators or possibly complex biosensors / see also 12,14 /.

Appendix

Calculation of the linear driving force

Consider the situation illustrated in the Fig.A1 and assume that by the field, which is of the form

$$\mathbf{E}=\mathbf{E}(r,t), \tag{a1}$$

only a dipole moment (p) is induced on the sphere:

$$\mathbf{p}=\mathbf{P}\mathbf{E} \quad (\mathbf{P}:\text{Polarization}) \tag{a2}$$

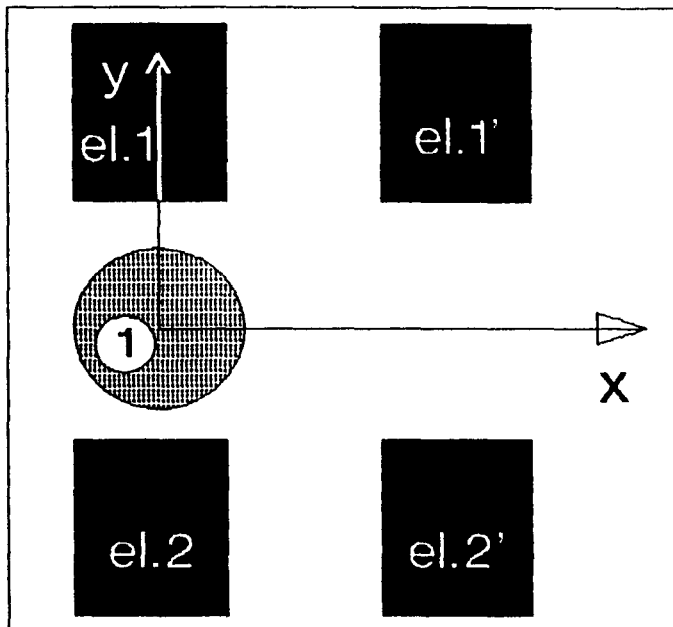


FIG.A1
Linear arrangement of electrodes, the force in x-direction is estimated.

If higher multipoles are neglected the force on the sphere would be of the form

$$\mathbf{F}=\mathbf{p}\nabla\mathbf{E}=\mathbf{P}\mathbf{E}\nabla\mathbf{E} \quad ; \tag{a3}$$

Even in this simple case it is practically impossible to calculate the field for an arrangement of electrodes as

used.

In order to estimate the field one could construct the external field by a superposition of point charges $q_i = q_i(r_i, t)$ where each point charge produces, within the sphere, a series of multipoles. This procedure is very expensive and is under investigation now.

To understand the general behaviour the calculation is restricted to the case shown in Fig.A2.

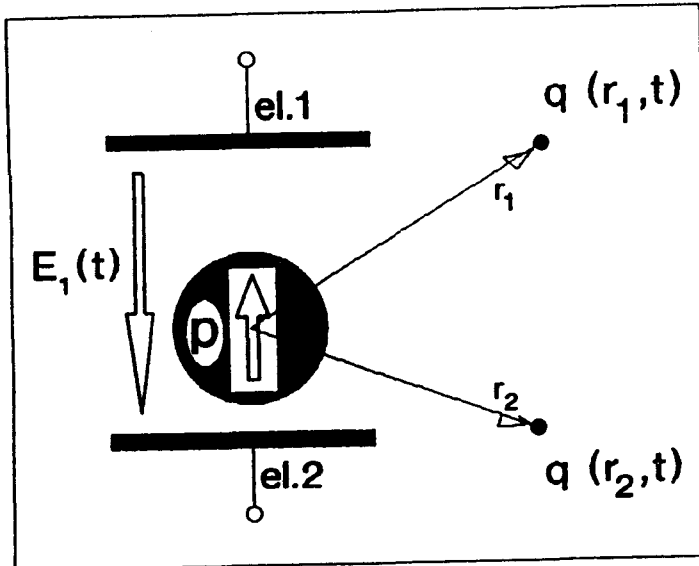


FIG.A2

The electrodes el.1/el.2, which induce a dipole of the form (a2), are excited by a sequence of rectangular pulses. The dipole (p) in turn produces a dipole-field $E_p(r, t)$. The both electrodes which are in neighbourhood of the electrodes el.1/el.2 (compare Fig.A1) are substituted by the point charges $q(r_1, t)$ and $q(r_2, t)$

The forces between the dipole (p) and the both charges are $F_1 = E_p(r_1, t)q(r_1, t)$ and $F_2 = E_p(r_2, t)q(r_2, t)$, respectively. These forces cause a lateral movement of the sphere: The field E_1 (generated by the electrodes el.1/el.2) is of the form $E_1(t) = E_1(t + 2T)$ where $2T$ is the period and

$$E_1(t) = \begin{cases} E_1, & 0 < t < T \\ -E_1, & T < t < 2T \end{cases} \quad (a4)$$

Within such a homogeneous field the time dependent dipole moment ($p(t)$) may be calculated by solving the equation

$$ap + \dot{p} = cE_1 + d\dot{E}_1 \quad (a5)$$

where the constants a , c and d are determined by the geometry of the dielectric particle. To obtain this equation one may solve the problem of a dielectric sphere within a constant field. The result, a relation between the external field and the dipole moment, depends on the real permittivities of both the sphere and the medium. To obtain from this the above equation, one has to replace the real permittivities by $\epsilon_1 \rightarrow \sigma_1 + \epsilon_1 \delta / \delta t$. In the case of a homogeneous sphere (ϵ_1, σ_1) immersed within a medium of permittivity ϵ_2 and conductivity σ_2 we find / 7,11 /:

$$a = (2\sigma_2 + \sigma_1) / (2\epsilon_2 + \epsilon_1); \quad c = K(\sigma_1 - \sigma_2) / (2\epsilon_2 + \epsilon_1)$$

$$d = K(\epsilon_1 - \epsilon_2) / (2\epsilon_2 + \epsilon_1); \quad K = 4\pi R^3 \epsilon_2. \tag{a6}$$

From (a5) the dipole is given by:

$$p(0 < t < T) = [1 - \exp(-at)] * cE_1/a + \exp(-at) * dE_1 \tag{a7}$$

$$p(T < t < 2T) = \{ 2\exp[-a(t-T)] - \exp(-at) - 1 \} * cE_1/a + \{ \exp(-at) - 2\exp[-a(t-T)] \} * dE_1$$

The component in x-direction of the time averaged force between the sphere and the both charges is of the form:

$$\langle F_x(t) \rangle = 1/2T \{ E_{x,p}(r_1, t) q_1(r_1, t) + E_{x,p}(r_2, t) q_2(r_2, t) \} dt \tag{a8}$$

Here $E_{x,p}(r_1, t)$ is the field that the dipole generates at the position of the both additional charges q_1 .

Solving this for the case that the charges $q_1(t) = -q_2(t)$ produces a field that is proportional to $E_1(t+T/2)$ (the phase shift of $T/2$ provides for an traveling excitation) we get the estimation:

$$\langle F_x \rangle = G(r) * (c/a-d) * [3 - \exp(-aT)] [\exp(-aT/2) - 1]^2 * E_1^2 / (2aT) \tag{a9}$$

Here the geometrical factor $G(r)$ depends only on the coordinates of the dipole.

The factor $(c/a-d)$ defines the direction of movement (see equ. (a6)), the frequency response is determined by the relaxation time $\tau = 1/a$ (see Fig.A3):

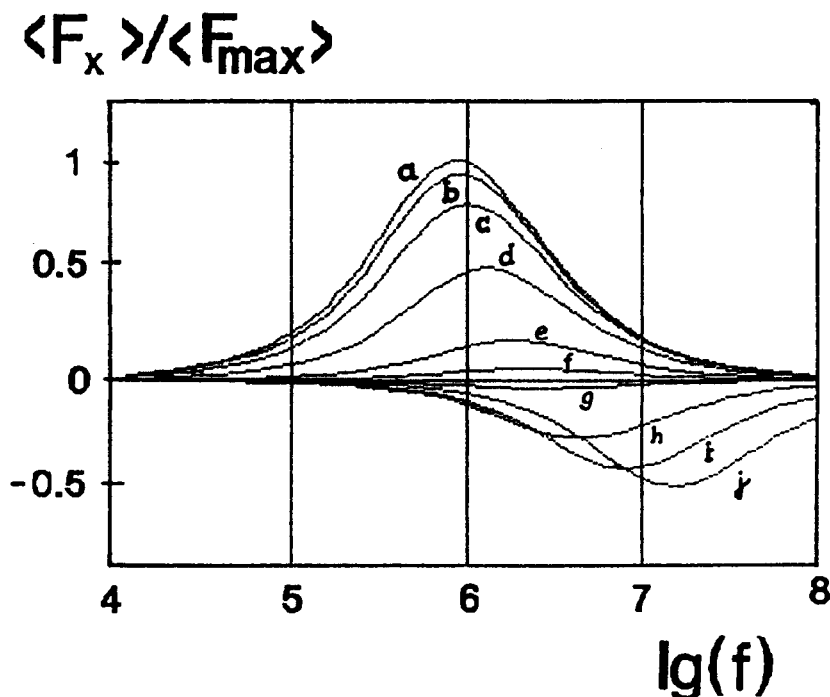


FIG.A3
 Frequency response of a homogeneous sphere with permittivity $\epsilon_1 = 70 * \epsilon_0$ and conductivity $\sigma_1 = 0.008$ S/m surrounded by a medium of permittivity $\epsilon_2 = 80 * \epsilon_0$. The conductivity of the medium (σ_2) varies between 0.0008 (curve (a)) and 0.08 (curve (j))

Acknowledgement

We are grateful to Mrs. Streck for writing this manuscript.

References

- /1/ ARNOLD, W.M. and ZIMMERMANN, U., Z. Naturforsch. 37, (1982), 908
- /2/ CROWLEY, J.U., J. Electrostatics 8, (1980), 171
- /3/ FUHR, G., GLASER, R. and HAGEDORN, R., Biophys. J. 49, (1986), 395
- /4/ FUHR, G., HAGEDORN, R. and GÖRING, H., Plant Cell Physiol. 26, (1985), 1527
- /5/ JONES, T.B., IEEE Trans. IAS, Vol. IA-21, (1985), 930
- /6/ KALER, K.V.I.S. and JONES, T.B., Biophys. J. 57, (1990), 173
- /7/ LAMPA, A., Sitzungsber. der K. Akad. Wiss. 115, (1906) 1659
- /8/ MASUDA, S., WASHIZU, M. and KAWABATA, I., IEEE Transactions on Industry Applications 24, (1988), 217
- /9/ MASUDA, S., WASHIZU, M. and IWADARE, M., IEEE Transactions on Industry Applications IA-23, (1987), 474
- /10/ MELCHER, J.R., The Physics of Fluids 9, (1966), 1548
- /11/ POHL, H.A., Dielectrophoresis, Cambridge University Press, New York (1978)
- /12/ SATO, K., KAMAMURA, Y., TANAKA, S., UCHIDA, K. and KOHIDA, H., Sensors and Actuators A 21 - A 23, (1990), 948
- /13/ SAUER, F. A., "Interaction forces between microscopic particles in an external electromagnetic field", in: Interactions between Electromagnetic Fields and Cells A. Chiabrera, C. Nicolini and H. Schwan (eds.), Plenum Pub. Corp., New York, (1985), 181
- /14/ WASHIZU, U., Electrostatic manipulation of biological objects in microfabricated structures, 3. Toyota Conference, Oct. '89, (25-1), (1989)
- /15/ ZIMMERMANN, U. and VIENKEN, J., J. Membr. Biol. 67, (1982), 165

Received on 20. 2. 1991

Dr. G. FUHR, Humboldt-University of Berlin, Invalidenstr. 42,
O-1040 Berlin, Germany